Instability of Compressible Boundary Layers Along Curved Walls with Suction or Cooling

Nabil M. El-Hady* and Alok K. Verma†
Old Dominion University, Norfolk, Virginia

This paper investigates the effect of suction of the boundary layer and wall cooling on the growth and development of three-dimensional longitudinal vortices over concave walls. The study is carried out for compressible flows for a range of Mach numbers of 0-5. Despite indications that low suction or low cooling rates locally reduce the critical Görtler number (destabilize the boundary layer), the overall effect of suction or cooling is to stabilize the boundary layer by reducing the amplitude ratio of the vortices. In case of suction, this becomes more difficult as the Mach number increases unless high suction rates are used. On the other hand, stabilizing the boundary layer with respect to the Görtler vortices can hardly be achieved by cooling, even when high cooling rates are used.

Introduction

IT is known that the flow on a concave wall exhibits a strong inviscid instability under the influence of centrifugal forces induced by curvature effects. This instability may produce a three-dimensional system of counterrotating vortices with axis in the streamwise direction, commonly referred to as Görtler vortices. On the other hand, Tollmien-Schlichting (TS) or cross-flow (CF) instabilities are expected to behave on a concave wall in almost the same way as on a flat plate because the effect of wall curvature (likely to occur in practice) is very small.

Available experimental evidence has shown that the effect of Görtler vortices on boundary-layer transition on a concave wall is rather indirect. They are responsible for inducing a spanwise variation of the velocity field, thus modifying the development of unstable (TS or CF) waves.

Suction of the boundary layer or wall cooling are means that can be used in a laminar flow control (LFC) system to delay transition of the laminar airflow. In such LFC systems, all types of flow instabilities may exist, including TS, CF, and Görtler vortices. Available theoretical results indicate that low suction or cooling rates may be used to totally stabilize the boundary layer with respect to TS instabilities, while for CF instabilities higher suction or cooling rates are required for the same purpose. It is the aim of this work to study the effect of suction or cooling on Görtler vortices.

Kobayashi[1-3] was the first to examine the effect of suction on the stability characteristics of a laminar incompressible boundary layer along a curved surface. Although his analysis excluded the effect of the normal component of the mean velocity due to boundary-layer growth, it gave insight into the effect of the presence of this velocity component due to suction. Using homogeneous suctions Kobayashi found that the laminar boundary layer is stabilized (critical Görtler number increases). However, the changes in the critical Görtler number remain much less than the changes in the critical Reynolds number for the TS instabilities due to homogeneous suction according to Hughes and Reid.[4] Hence, Görtler instability will probably predominate in the laminar boundary layer along the concave wall with suction. Floryan and Saric[5,6] included the normal component of the mean velocity in their analysis and examined the case of self-similar suction and came to the same conclusion.

Diprima and Dunn[7] examined the effect of cooling and heating on the stability characteristics of laminar liquid boundary layer over a curved surface. Since their analysis was made on liquids, they neglected the viscous dissipation and variations in density and came to a conclusion that heating or cooling has very slight influence on Görtler instability. For compressible boundary layers, Kobayashi and Kohama[8] found that for isothermal walls the ratio of the wall-to-freestream temperatures has less effect on the critical value of the Görtler number as the Mach number increases.

In this paper, we investigate the effect of suction of the boundary layer or wall cooling on the development of Görtler vortices at different Mach numbers. In the analysis we use the compressible linear stability theory introduced by El-Hady and Verma[9] for the development of three-dimensional longitudinal vortices along curved walls.

Problem Formulation

Consider the spatial three-dimensional stability of laminar compressible two-dimensional boundary layers along a slightly curved wall. The wall curvature is in the direction of the flow and its variation is assumed to be weak to avoid a nonuniform Mach number distribution along the wall due to the presence of shock waves that might occur in the case of rapid changes. The flowfield is governed by the Navier-Stokes, energy, continuity, and state equations written in an orthogonal curvilinear coordinate system. The local curvature of the streamlines enters the field equations through the appropriate coordinate system. Here, we follow Floryan and Saric[5] and use a coordinate system (x,y,z) based on the streamlines and potential lines of the inviscid flow over a curved surface, where x and y are in the direction of streamlines and potential lines, respectively, and z is the coordinate normal to the x-y plane. The local curvature of the streamlines enters the field equations through the metric coefficients. They are determined from the definition of the arc length to be h, h, and 1 in the x, y, and z directions, respectively. The field equations are used to formulate the disturbance equations. These equations, written in the specified coordinate system, and the detailed formulation of the problem are presented elsewhere.[9] The following presentation is limited to a short outline.

Presented as Paper 82-1010 at the AIAA/ASME Third Joint Thermophysics, Fluids, Plasma and Heat Transfer Conference, St. Louis, Mo., June 7-11, 1982; submitted June 17, 1982; revision received April 12, 1983. This paper is declared a work of the U.S. Government and therefore is in the public domain.

*Assistant Professor, Department of Mechanical Engineering and Mechanics (presently with Department of Engineering Mathematics, King Abdulaziz University, Jeddah, Saudi Arabia). Member AIAA.

†Graduate Student, Department of Mechanical Engineering and Mechanics (presently, Assistant Professor, Department of Mechanical Engineering Technology).

We consider the basic state to be two-dimensional, viscous, compressible flow over a slightly curved surface. The field equations are made dimensionless using a reference length

$$L^* = (\nu_\infty^* x^* / U_\infty^*)^{1/2} \tag{1}$$

U_∞^* as a reference velocity, and $\rho_\infty^* U_\infty^{*2}$ as a reference pressure, where * indicates a dimensional quantity and ν is the kinematic viscosity of the fluid. The thermodynamic and transport properties of the fluid are made dimensionless using their corresponding freestream values. With these definitions, the characteristic Reynolds number becomes

$$R = (U_\infty^* L^* / \nu_\infty^*) \tag{2}$$

We define a small viscous parameter ϵ and a small curvature parameter k as

$$\epsilon = 1/R, \qquad k = (L^* K^*)^{1/2} \tag{3}$$

where K^* is the curvature of the wall. The metric coefficient h is related to the curvature parameter k by

$$k^2 = -h_y / h^2 \quad \text{at} \quad y = 0 \tag{4}$$

where the subscript y denotes $\partial/\partial y$.

Because the aim of this study is to provide a basic approximation for the stability of a compressible boundary layer over a curved surface, a basic approximation of the mean flow is required. When the small parameters ϵ and k are of the same order, the basic approximation of the boundary-layer equations is the conventional compressible flow over a flat plate. Mean flow profiles are calculated for an adiabatic or isothermal flat plate. In case of suction, we define a similar suction parameter γ as

$$\gamma = (\rho_w^* v_w^* / \rho_\infty^* U_\infty^*) R \tag{5}$$

and introduce it to the boundary-layer equations. Here w indicates wall conditions and R is given in Eq. (2). The fluid is considered to be a perfect gas with all the thermodynamic and transport property functions of temperature. The mean viscosity is related to the mean temperature through the Sutherland formula. The flow stagnation temperature is kept constant and equal to 310 K for all of the Mach numbers under study.

For the stability analysis, steady three-dimensional small-disturbance quantities are made dimensionless using

$$u = u^*/U_\infty^*, \qquad v = v^*/RU_\infty^*, \qquad w = w^*/RU_\infty^*$$
$$p = p^*/R^2 \rho^* U_\infty^{*2}, \qquad \theta = \theta^*/\Theta_\infty^*, \qquad \rho = \rho^*/\bar{\rho}_\infty^* \tag{6}$$

and are superposed on the mean flow velocities U and V, pressure P, temperature Θ, density $\bar{\rho}$, and viscosity μ, in the following form:

$$\hat{u}(x,y,z) = U(x,y) + u(x,y,z) \tag{7a}$$

$$\hat{v}(x,y,z) = V(x,y) + v(x,y,z) \tag{7b}$$

$$\hat{w}(x,y,z) = 0 + w(x,y,z) \tag{7c}$$

$$\hat{p}(x,y,z) = P(x,y) + p(x,y,z) \tag{7d}$$

$$\hat{\Theta}(x,y,z) = \Theta(x,y) + \theta(x,y,z) \tag{7e}$$

$$\hat{\rho}(x,y,z) = \bar{\rho}(x,y) + \rho(x,y,z) \tag{7f}$$

$$\hat{\mu}(x,y,z) = \mu(\Theta) + (\mathrm{d}\mu/\mathrm{d}\Theta)\theta(x,y,z) \tag{7g}$$

With the scaling given by Eq. (6), the disturbance motion varies in the x coordinate according to the slow scale,[9] $x = x^*/RL^*$. Boundary-layer theory, combined with the assumed scales, gives the x variation of the mean flow in terms of the slow scale x.

Substituting Eqs. (7) into the dimensionless field equations, subtracting the mean flow, linearizing the equations, and keeping the leading-order terms, that is, terms 0(1), the following disturbance equations are obtained:

x momentum

$$(1/\Theta)(Uu)_x + (V/\Theta)u_y - (\mu u_y)_y - \mu u_{zz} + (1/\Theta)U_y v - [(1/\Theta^2)(UU_x + VU_y) + (\tilde{\mu}U_y)_y]\theta - \mu U_y \theta_y = 0 \tag{8}$$

y momentum

$$(1/\Theta)(V_x + 2UG^2)u - c\mu_y u_x - (c+1)\mu u_{yx} - \mu_x u_y + (1/\Theta)(Vv)_y + (U/\Theta)v_x - \mu v_{zz} - (c+2)(\mu v_y)_y - c\mu_y w_z - (c+1)\mu w_{yz} + p_y - [(1/\Theta^2)(UV_x + VV_y + U^2G^2) + (c+1)\tilde{\mu}U_{yx} + c\tilde{\mu}_y U_x + \tilde{\mu}_x U_y + (c+2)(\tilde{\mu}V_y)_y]\theta - \tilde{\mu}U_y\theta_x - [c\tilde{\mu}U_x + (c+2)\tilde{\mu}V_y]\theta_y = 0 \tag{9}$$

z momentum

$$\mu_x u_z + (c+1)\mu u_{xz} + \mu_y v_z + (c+1)\mu v_{yz} - (1/\Theta)(Uw_x + Vw_y) + (\mu w_y)_y + (c+2)\mu w_{zz} - p_z + c\tilde{\mu}(U_x + V_y)\theta_z = 0 \tag{10}$$

continuity

$$\left(\frac{u}{\Theta}\right)_x + \left(\frac{v}{\Theta}\right)_y + \left(\frac{w}{\Theta}\right)_z + \frac{1}{\Theta^2}\left(\frac{2U}{\Theta}\Theta_x + \frac{2V}{\Theta}\Theta_y - U_x - V_y\right)\theta - \frac{1}{\Theta^2}(U\theta_x + V\theta_y) = 0 \tag{11}$$

energy

$$\frac{1}{\Theta}\Theta_x u - 2(\tilde{\gamma}-1)M_\infty^2 \mu U_y u_y + \frac{1}{\Theta}\Theta_y v - \left[\frac{1}{\Theta^2}(U\Theta_x + V\Theta_y) + (\tilde{\gamma}-1)M_\infty^2 \tilde{\mu}(U_y)^2 + \frac{1}{\Gamma}\mu_{yy}\right]\theta + \frac{U}{\Theta}\theta_x - \frac{\mu}{\Gamma}\theta_{zz} + \left(\frac{V}{\Theta} - \frac{2}{\Gamma}\mu_y\right)\theta_y - \frac{1}{\Gamma}\mu\theta_{yy} = 0 \tag{12}$$

At this level of approximation, Eqs. (8-12) are configuration independent because the parameters ϵ and k appear only implicitly in the so-called Görtler number G, which is defined by

$$G = Rk \tag{13}$$

Other parameters appearing in Eqs. (8-12) are the freestream Mach number M_∞, Prandtl number Γ, the ratio $\tilde{\gamma}$ of the perfect gas specific heats, and $\tilde{\mu} = \mathrm{d}\mu/\mathrm{d}\Theta$. The ratio c of the second to the first mean flow viscosity coefficient is defined as $c = 2(e-1)/3$, e being equal to 0.8. The density disturbance is eliminated by using the equation of state. The subscripts x, y, and z refer to $\partial/\partial x$, $\partial/\partial y$, and $\partial/\partial z$, respectively. Equations

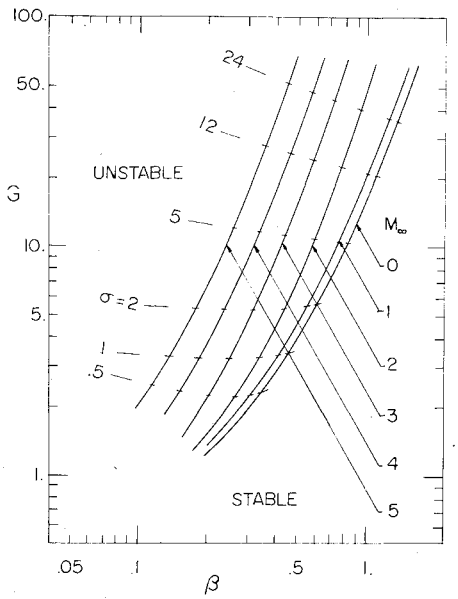

Fig. 1 Effect of compressibility on the locus of maximum growth rates.

(8-12) are supplemented with the appropriate boundary conditions,

$$u=v=w=0 \quad \text{and} \quad \theta_y+B\theta=0 \quad \text{at} \quad y=0 \tag{14}$$

$$u,v,w,\theta \to 0 \qquad \text{as} \quad y\to\infty \tag{15}$$

The function B in Eqs. (14) depends on the thermal properties of both the solid surface and the fluid, as well as the wavelength of the disturbance. Local stability near the neutral region is dependent on the wall boundary condition of the thermal disturbance.[9] The effect of this thermal condition vanishes with the growth of the disturbance. In case of suction, we consider the wall to be adiabatic and take $B\to 0(\theta_y=0$ at $y=0)$. However, for cases involving wall cooling, we take $B\to\infty(\theta=0$ at $y=0)$. Equations (15) express the physical fact that the disturbances may decay in the freestream.

The disturbances under consideration are assumed in the form of

$$u=\hat{u}(y)\cos(\beta z)\exp(\int\sigma dx) \tag{16a}$$

$$v=\hat{v}(y)\cos(\beta z)\exp(\int\sigma dx) \tag{16b}$$

$$w=\hat{w}(y)\sin(\beta z)\exp(\int\sigma dx) \tag{16c}$$

$$p=\hat{p}(y)\cos(\beta z)\exp(\int\sigma dx) \tag{16d}$$

$$\theta=\hat{\theta}(y)\cos(\beta z)\exp(\int\sigma dx) \tag{16e}$$

where β is the dimensionless wavenumber in the z coordinate and σ the spatial growth rate.

Computational and Numerical Procedures

Substituting Eqs. (16) into Eqs. (8-12), we obtain an eighth-order system of homogeneous linear ordinary differential equations. This forms an eigenvalue problem for the parameters β,σ, and G. Using the notation

$$Z_1=\hat{u}, \quad Z_2=D\hat{u}, \quad Z_3=\hat{v}, \quad Z_4=\hat{p}$$

$$Z_5=\hat{\theta}, \quad Z_6=D\hat{\theta}, \quad Z_7=\hat{w}, \quad Z_8=D\hat{w} \tag{17}$$

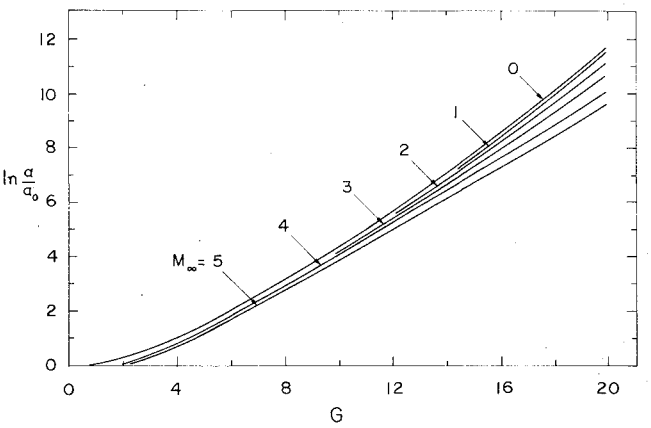

Fig. 2 Effect of compressibility on the amplitude ratios calculated along the locus of maximum growth rates.

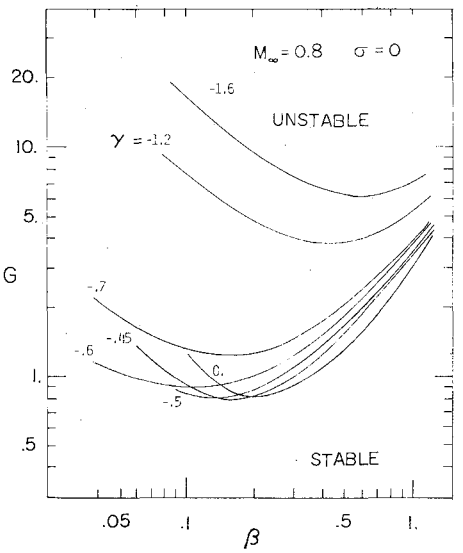

Fig. 3 Neutral stability curves for different values of the suction parameter at $M_\infty=0.8$.

we write the system of Eqs. (8-12) in the compact form

$$DZ_m-\sum_{n=1}^{8}a_{mn}Z_n=0, \qquad m=1,2,\ldots,8 \tag{18}$$

$$Z_1=Z_3=Z_7=0 \quad \text{and} \quad Z_5=0 \quad \text{or} \quad Z_6=0 \quad \text{at} \quad y=0 \tag{19}$$

$$Z_1,Z_3,Z_5,Z_7\to 0 \qquad \text{as} \quad y\to\infty \tag{20}$$

where $D=\mathrm{d}/\mathrm{d}y$ and a_{mn} are the elements of the 8×8 variable-coefficient matrix whose nonzero elements are given in the Appendix. The condition $Z_5=0$ at $y=0$ is used for isothermal wall, while $Z_6=0$ at $y=0$ is used for adiabatic wall.

Outside the boundary layer, i.e., at $y>y_e$ (e indicates the edge of the boundary layer), the coefficients in Eqs. (18) become constant. With the constant coefficient matrix, Eqs. (18) have a solution that can be expressed in the form

$$Z_m=\sum_{n=1}^{8}d_{mn}c_n\exp(\lambda_n y), \quad m=1,2,\ldots 8; \quad y=y_e \tag{21}$$

where d_{mn} is the characteristic eigenvector matrix, c_n the arbitrary constant vector, and λ_n the eigenvalues of the

constant coefficient matrix, which are

$$\lambda_1 = -\beta \tag{22a}$$

$$\lambda_2 = \lambda_3 = -\tfrac{1}{2}\{-V_e + [V_e^2 + 4(\sigma+\beta^2)]^{1/2}\} \tag{22b}$$

$$\lambda_4 = -\tfrac{1}{2}\{-\Gamma_e V_e + [\Gamma_e^2 V_e^2 + 4(\sigma\Gamma_e + \beta^2)]^{1/2}\} \tag{22c}$$

$$\lambda_5 = \beta \tag{22d}$$

$$\lambda_6 = \lambda_7 = \tfrac{1}{2}\{V_e + [V_e^2 + 4(\sigma+\beta^2)]^{1/2}\} \tag{22e}$$

$$\lambda_8 = \tfrac{1}{2}\{\Gamma_e V_e + [\Gamma_e^2 V_e^2 + 4(\sigma\Gamma_e + \beta^2)]^{1/2}\} \tag{22f}$$

We consider the case in which λ_1, λ_2, λ_3, and λ_4 are negative real numbers, whereas the other four are positive real numbers. Only negative signs satisfy the boundary conditions of Eqs. (15) as $y \to \infty$. This demands that the constants c_5-c_8 be zeros in Eq. (21) and is expressed as

$$\sum_{n=1}^{8} d_{mn}^{-1} Z_n = 0, \qquad m = 5,6,7,8; \quad y = y_e \tag{23}$$

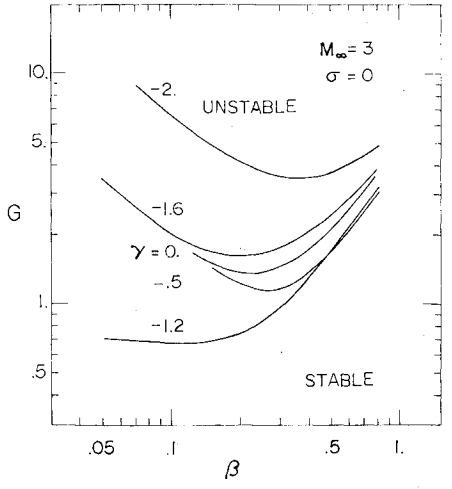

Fig. 4 Neutral stability curves for different values of the suction parameter at $M_\infty = 3$.

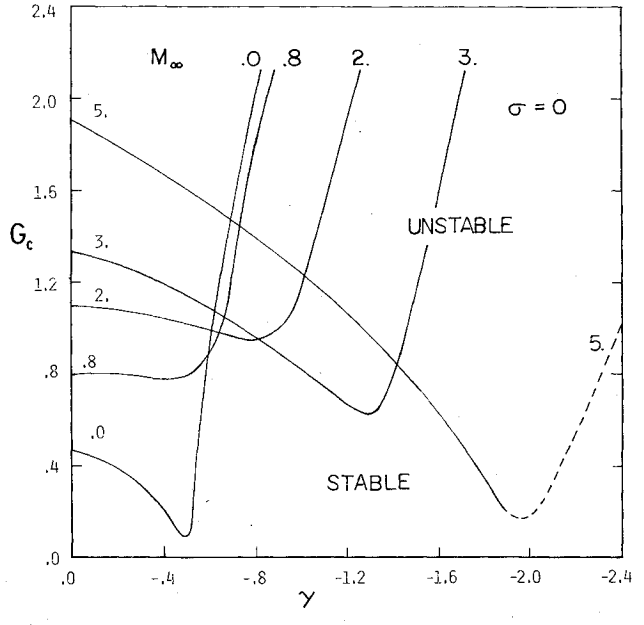

Fig. 5 Effect of suction on the critical Görtler number for different Mach numbers.

The boundary condition at the wall [Eq. (19)] can be written in the form

$$\sum_{n=1}^{8} e_{mn} Z_n = 0, \qquad m = 1,2,3,4; \; y = 0 \tag{24}$$

where the elements of the 4×8 matrix e_{mn} are all zeros except $e_{11} = e_{23} = e_{36} = e_{47} = 1$ in the case of an adiabatic wall and $e_{11} = e_{23} = e_{35} = e_{47} = 1$ in the case of an isothermal wall.

Equations (18) with the boundary conditions of Eqs. (23) and (24) form a two-point boundary value problem that is solved numerically using a forward integration routine.[10] We assign values for two of the parameters β, σ, and G, guess the third one, and use Eq. (23) to construct a linear combination of the general solution [Eq. (21)]. We integrate Eqs. (18) from $y = y_e$ to the wall. At the wall, the values of the independent solution vectors are linearly combined to satisfy all but one of the wall boundary conditions. The last wall boundary condition can be satisfied by this combined solution only when the exact eigenvalue has been found. A Newton-Raphson procedure is used to determine this value.

The system of equations adjoint to Eqs. (18) are formed to check the eigenvalues. The adjoint system can be written as

$$DZ_m^* + \sum_{n=1}^{8} a_{nm} Z_n^* = 0, \qquad m = 1,2,\ldots,8 \tag{25}$$

$$Z_2^* = Z_4^* = Z_8^* = 0 \quad \text{and} \quad Z_5^* = 0 \quad \text{or} \quad Z_6^* = 0 \quad \text{at} \quad y = 0 \tag{26}$$

$$Z_2^*, Z_4^*, Z_6^*, Z_8^* \to 0 \qquad \text{as} \quad y \to \infty \tag{27}$$

where the homogeneous boundary condition $Z_5^* = 0$ at $y = 0$ is used for the adiabatic wall while $Z_6^* = 0$ at $y = 0$ is used for the isothermal wall. Equations (25-27) are solved with the same procedure used to solve the regular equations (18-20). Eigenvalues calculated by Eqs. (18) and their adjoint [Eq. (25)] were checked and found to agree to $0(10^{-4})$, and both were found to be independent of the value of y_e. The shape of the eigenfunctions was also checked in order to avoid calculations of higher modes.

Effect of Compressibility

Stability results are usually presented as constant growth rate curves of Görtler number vs wave number (G-β plane).

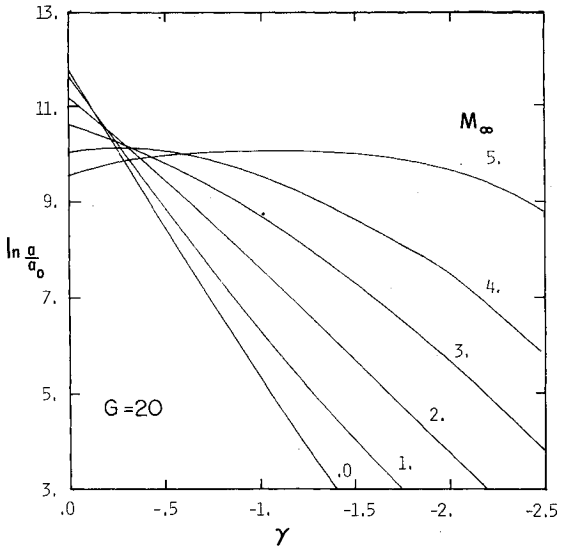

Fig. 6 Effect of suction on the amplitude ratios at $G = 20$ for different Mach numbers.

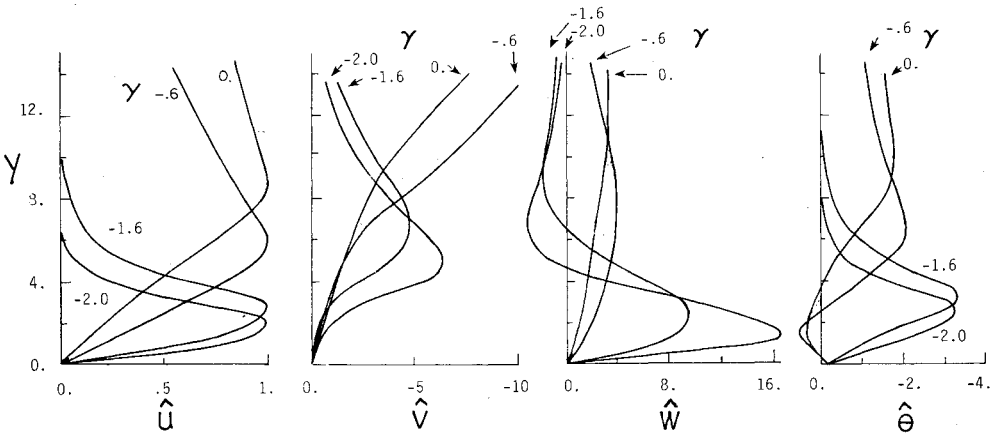

Fig. 7 Effect of suction at $M_\infty = 3$ on the shape of the eigenfunctions for a neutrally stable disturbance having a wave number of 0.3.

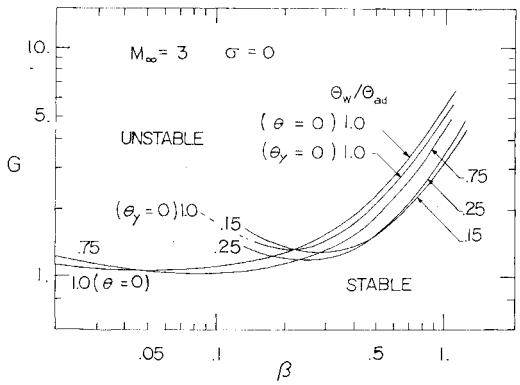

Fig. 8 Neutral stability curves for different cooling rates at $M_\infty = 3.0$.

The instability of the boundary layer sets in at a higher Görtler number as the Mach number increases for almost all wavelengths.[9] Compressibility has its maximum stabilizing influence when the vortex is weak. Growth rate curves possess minimums that move to higher wave numbers as the vortex grows. These minimums form the loci of the maximum growth rates of the different wave number components. Figure 1 indicates that as the Mach number increases, this locus shifts up and to the left in the G-β plane, that is, maximum growth rates occur at higher Görtler numbers and lower wave numbers. It can be detected from Fig. 1 that as the Mach number increases, the most unstable wavelength and the cutoff wavelength both shift to a higher value.[9]

The growth of the vortices measured by the amplitude ratio is calculated using

$$\ell n\left(\frac{a}{a_0}\right) = \frac{4}{3}\int_{G_0}^{G}\left(\frac{\sigma}{G}\right)dG \tag{28}$$

where a_0 and G_0 are the amplitude and Görtler number at the beginning of the unstable region, respectively, and the integration is carried along a particular growth path. The growth path of the vortex is determined by a wavelength selection mechanism.[6] The stability theory cannot predict which disturbance wavelength will actually appear for a given surface configuration and flow condition. The wavelength selection mechanism may be based on the maximum growth rate of the disturbance (then the growth path is the locus of maximum growth rates) or may be based on the most unstable wavelength defined by the dimensionless parameter

$$\Lambda = (U_\infty^* \lambda^*/\nu_\infty^*)\,(\lambda^* K^*)^{1/2} \tag{29}$$

(then the growth path is determined from the conservation of the most unstable λ^*). In the G-β plane, $\Lambda = \text{const}$ are straight lines with 3/2 slopes that closely coincide with the loci of the maximum growth rates for the corresponding Mach numbers.

For different Mach numbers, Fig. 2 shows the result of integrating Eq. (28) along the loci of the maximum growth rates. The integration is carried up to $G = 20$ for comparison purposes. The figure shows a stabilizing effect as the Mach number increases in terms of lower values of $\ell n(a/a_0)$. El-Hady and Verma[9] showed that by following the growth path of the most unstable wavelength (corresponding to each Mach number), the values of $\ell n(a/a_0)$ at $G = 20$ for different Mach numbers are identical to the corresponding values in Fig. 2.

Effect of Suction

It was shown by Görtler[11] and Hämmerlin[12] that the curve of neutral stability depends insensibly upon the basic velocity profile in the laminar incompressible boundary layer when the changes in its momentum thickness are very small. However, Kahawita and Meroney[13] showed that the inclusion of the normal velocity terms in the basic flow changes the location of the neutral curve drastically. El-Hady and Verma[9] reached the same conclusion for the compressible boundary layer. Terms due to boundary-layer growth have a large effect near the neutral stability region especially at high Mach numbers. Therefore, it is expected that variations of the velocity profile due to suction (which does not affect the momentum thickness but changes the normal velocity term) may change the critical Görtler number.

The effect of the suction of the laminar boundary layer on Görtler instability is examined at $M_\infty = 0.8$ and 3. The self-similar suction parameter γ defined in Eq. (5) is used for this purpose. Figures 3 and 4 show the change in the location of neutral stability curves for different values of the suction parameter at $M_\infty = 0.8$ and 3, respectively. It is observed that the critical Görtler number first decreases with increasing suction (destabilizing the boundary layer). The boundary layer with a suction given by $\gamma \simeq -0.45$ at $M_\infty = 0.8$ or $\gamma \simeq -1.3$ at $M_\infty = 3$ is the most unstable as far as the critical Görtler number is concerned. By increasing the suction parameter above these levels for each Mach number, the critical Görtler number increases. Figure 5 shows how the critical Görtler number changes with γ for different Mach numbers. The level of suction required for a noticeable increase in the critical Görtler number increases as the Mach number increases. This suction level is an order of magnitude higher than the suction level required to stabilize TS instabilities (see Saric and Nayfeh[14] for $M_\infty = 0$), and is almost the same order of magnitude of the suction level required to stabilize CF instabilities (see El-Hady[15] for $M_\infty = 0.8$). This leads to the conclusion that, with these levels of suction, TS instabilities are practically eliminated and CF and/or Görtler vortices may dominate the flow.

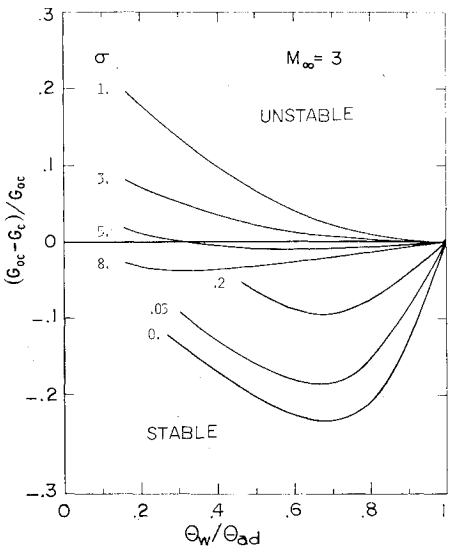

Fig. 9 Effect of wall cooling on local stability at $M_\infty = 3.0$.

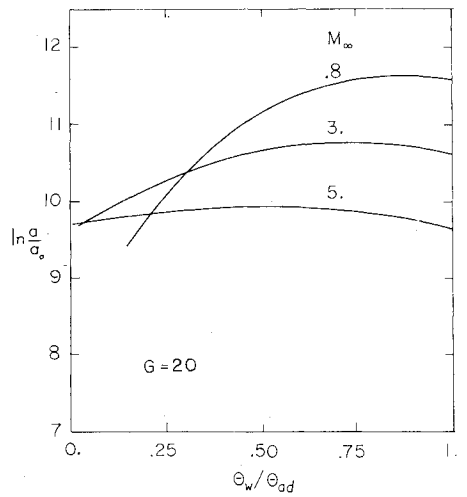

Fig. 10 Effect of wall cooling on the amplitude ratios at $G = 20$ for different Mach numbers.

By increasing the suction, the curves of constant growth rates in the G-β plane are compressed and moved to higher Görtler numbers. Curves of high growth rates are less affected by suction, especially at high Mach numbers. To see the overall effect of suction, the growth of the vortices should be taken into account as they develop downstream. Integration of growth rates using Eq. (28) is performed along the loci of maximum growth rates to $G = 20$ for comparison purposes. For different Mach numbers, Fig. 6 displays the amplitude ratio of the vortices at $G = 20$ for a range of the suction parameter γ. It is clear that despite indications of a destabilizing effect of low suction for all Mach numbers regarding the critical Görtler number (see Fig. 5), the overall effect of suction is to stabilize the boundary layer as shown by Fig. 6. Although a suction corresponding to $\gamma = -1.2$ (which is near to the critical level of the suction parameter at $M_\infty = 3$) locally destabilizes the boundary layer in terms of the critical Görtler number, it reduces the amplitude ratio by about 22%, thus stabilizing the boundary layer. The amplitude ratio of the vortices reduces as the suction increases. With increasing Mach number, it becomes more difficult to stabilize the boundary layer (reducing the amplitude ratio of the vortices) unless very high suction is used. Figure 6 shows that at $M_\infty = 5$ the amplitude ratio is hardly influenced by suction in the range of $0 < \gamma < -2$.

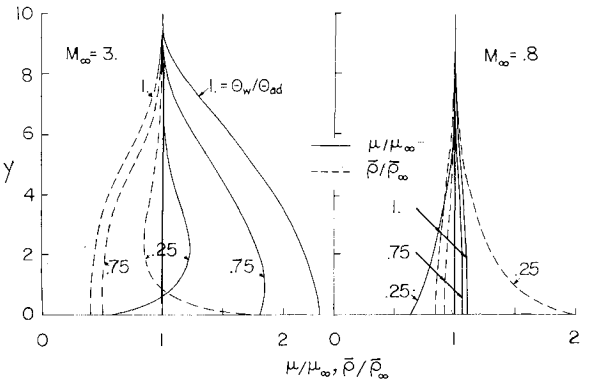

Fig. 11 Variation of the mean density and mean viscosity for different cooling rates at $M_\infty = 0.8$ and 3.

At $M_\infty = 3$, Fig. 7 shows a comparison of the shape of the eigenfunctions $\hat{u}$, $\hat{v}$, $\hat{w}$, and $\hat{\theta}$ normalized with the maximum of the $\hat{u}$ component for different values of the suction parameter γ. These eigenfunctions are for a neutrally stable disturbance having a wave number $\beta = 0.3$. Corresponding Görtler numbers are $G = 1.6124$, 1.1155, 1.7549, and 3.5193 at $\gamma = 0.0$, -0.6, -1.6, and -2.0, respectively. Figure 7 shows that the location of the maxima of $\hat{u}$ and $\hat{w}$ and the minima of $\hat{v}$ and $\hat{\theta}$ move toward the wall as the suction increases. When the normal velocity component of the basic flow is directed away from the wall (the case of no suction), it tends to destabilize the flow by encouraging penetration into the freestream where viscous dissipation is small. By increasing suction, the thickness of the boundary layer decreases, and the disturbance is confined to a region closer to the wall where dissipative action is strong, thereby increasing the stability of the flow.

Effect of Wall Cooling

Figure 8 shows how the location of the neutral curve varies with different cooling rates at $M_\infty = 3$. The cooling parameter Θ_w/Θ_{ad} is used for this purpose, where $\Theta_w/\Theta_{ad} = 1$ represents no cooling, and $\Theta_w/\Theta_{ad} < 1$ represents cooling. Slight cooling has a destabilizing influence; however, as cooling increases, the neutral curve moves upward, indicating a stabilizing effect as far as the critical Görtler number is concerned. For wave numbers approximately greater than 0.4, Fig. 8 shows that wall cooling always destabilizes the boundary layer (the Görtler number decreases).

It should be noted here that El-Hady and Verma[9] concluded that the neutral stability curve is dependent on the wall boundary condition of the thermal disturbance. Therefore, one may think it somewhat misleading to compare neutral curves in the case of cooling (where the wall is considered completely conducting and the wall boundary condition of the thermal disturbance is $\theta = 0$) with curves in the case of no cooling (where the wall is considered ideally insulated and the wall boundary condition of the thermal disturbance is $\theta_y = 0$). For this reason the neutral stability curve is recalculated for the no cooling case with the thermal wall boundary condition $\theta = 0$ and is shown in Fig. 8 for comparison. It is clear that previous conclusions regarding the effect of cooling on the critical Görtler number are valid.

Figure 9 displays the influence of cooling at $M_\infty = 3$ on the vortices at different stages of their growth. The parameter $(G_{oc} - G_c)/G_{oc}$ is used as the ordinate to indicate the stabilizing or destabilizing effect (increase or decrease in the critical Görtler number) as cooling increases compared with G_{oc}, the critical Görtler number at $\Theta_w/\Theta_{ad} = 1$ (no cooling) for the same value of the growth rate σ. Figure 9 shows that at $M_\infty = 3$, weak vortices (low growth rates) are more influenced by cooling. The cooling parameters $1 > \Theta_w/\Theta_{ad} > 0.75$ seem to destabilize the boundary layer. As cooling increases

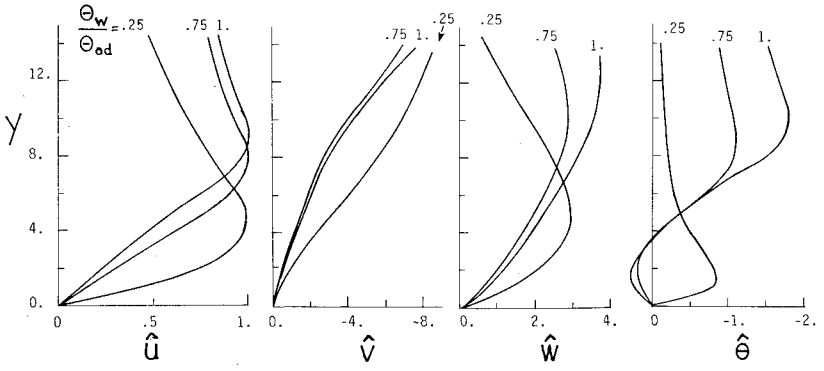

Fig. 12 Effect of wall cooling at $M_\infty = 3$ on the shape of eigenfunctions for a neutrally stable disturbance having a wave number of 0.3.

($\Theta_w/\Theta_{ad} < 0.75$), the figure shows a stabilizing influence of the cooling on weak vortices; however, cooling has almost no influence on strong vortices (high growth rates).

The above conclusions represent a local effect of cooling on the stability limit as well as growth rates of the vortices. It is important to estimate the effect of cooling on the total growth of the vortices by calculating the amplitude ratios. Again, we integrate the growth rates, using Eq. (28) along the loci of maximum growth rates to $G = 20$. Figure 10 shows the effect of cooling on the amplitude ratio of Görtler vortices for different Mach numbers. The figure demonstrates that moderate cooling has almost no influence on the stability regarding the amplitude ratio of the vortices. However, high cooling influences low Mach numbers. At the cooling rate $\Theta_w/\Theta_{ad} = 0.25$, the amplitude ratio is reduced by 13.4% at $M_\infty = 0.8$, by 2.8% at $M_\infty = 3$, and increased by 2.6% at $M_\infty = 5$.

The effect of moderate cooling, as shown in Fig. 10, is relatively small considering the strong temperature dependence of the viscosity and density and the corresponding large variation of both in the boundary layer. Figure 11 shows the distributions at $M_\infty = 0.8$ and 3 of the viscosity and density of the mean boundary-layer flow for different cooling parameters. In contrast to the insulated wall, where the density gradient is positive and the viscosity is large at the wall, the density profile for a high cooling rate may have both positive and negative gradients. The viscosity profile may also have two regions where $\mu > 1$ and $\mu < 1$. The negative density gradient may stabilize the flow according to the Rayleigh inviscid criterion, but the reduction in the effective viscosity in the boundary layer will have a destabilizing effect. It can, therefore, be said that the variation of both density and viscosity in moderate cooling cancel each other. On the other hand, in high cooling, stabilization of the boundary layer results because the effect of the negative density gradient is more predominant than the opposite effect of the reduction in the effective viscosity.

The effect of wall cooling on Görtler vortices as shown in Fig. 10 differs with the results for CF instabilities that are moderately sensitive to wall temperature (see Lekoudis[16] for $M_\infty = 0.8$). It is also in marked contrast to the results for TS instabilities that are extremely sensitive to wall temperature (see Fig. 7 in Mack[17] for $M_\infty = 3$). This is ultimately due to the presence of an inner critical layer in the TS disturbances through which the eigenfunction varies rapidly. Therefore, stability characteristics depend critically on the local properties of the mean flow velocity, viscosity, and density distribution that are very sensitive to the wall temperature. For Görtler instability, however, there is no inner critical layer and the centrifugal force is the controlling factor. This instability depends only on the overall properties of the mean flow, such as the average velocity gradient, that are much less influenced by the wall temperature.

Figure 12 gives a comparison of the shape of the eigenfunctions of $\hat{u}$, $\hat{v}$, $\hat{w}$, and $\hat{\theta}$ at $M_\infty = 3$ for different values of the cooling parameter Θ_w/Θ_{ad}. These eigenfunctions are for a neutrally stable disturbance with a wave number $\beta = 0.3$. Corresponding Görtler numbers are $G = 1.463$, 1.301, and 1.213 for $\Theta_w/\Theta_{ad} = 1.0$, 0.75, and 0.25, respectively. The values of $\hat{u}$, $\hat{v}$, $\hat{w}$, and $\hat{\theta}$ are normalized with the maximum of $\hat{u}$ component at the corresponding cooling parameter. The figure shows that the locations of the maxima of $\hat{u}$, $\hat{w}$ and the minimum of $\hat{\theta}$ move toward the wall as cooling increases. The velocity component $\hat{v}$ shows a persistance outside the boundary layer.

Conclusions

The influence of suction of the boundary layer or wall cooling on Görtler instability is investigated. The compressible stability theory introduced by El-Hady and Verma[9] for the boundary-layer flow along a concave wall is used in the analysis. The compressible boundary-layer equations along a flat plate with suction or cooling are used to represent the mean flow. The results of the stability analysis are summarized as follows:

1) Suction rates below a critical level may have a local destabilizing effect on the boundary layer as far as the critical Görtler number is concerned. This critical level of suction increases with Mach number.

2) In contrast with local suction effects, suction of the boundary layer has always a stabilizing influence on the total growth of Görtler vortices. The amplitude ratios of the vortices reduce with any level of suction used.

3) Suction of the boundary layer is more effective in stabilizing the flow at low Mach numbers than at high Mach numbers. It becomes increasingly difficult as Mach number increases to reduce the amplitude ratios of the vortices unless very high levels of suction are used.

4) Wall cooling, like suction, has a local destabilizing effect on the boundary layer as far as the critical Görtler number is concerned.

5) At low Mach numbers, cooling applied to the wall with the rate of $\Theta_w/\Theta_{ad} \geq 0.75$ has no influence on the amplitude ratios of Görtler vortices. A noticeable reduction in the amplitude ratio starts with cooling rates $\Theta_w/\Theta_{ad} \leq 0.5$.

6) At high Mach numbers, it seems almost impossible to stabilize the boundary layer using practical rates of wall cooling. The amplitude ratios of the vortices increase and the boundary layer becomes more unstable with rates of cooling $\Theta_w/\Theta_{ad} \geq 0.5$.

7) Comparing the shape of the eigenfunctions due to cooling in Fig. 12 with that due to suction in Fig. 7 shows that at $M_\infty = 3$, both high suction and high cooling stabilize the boundary layer by confining the disturbance to a highly dissipative region nearer to the wall. Suction may be more effective than cooling as it brings the disturbances closer to the wall.

8) Görtler instability is more difficult to influence and control by suction or cooling than Tollmien-Schilichting or cross-flow instabilities. The reason is that Görtler instability, which is referred to as a centrifugal-type instability, depends on the velocity difference between the inner and outer region of the boundary layer and not on the shape of the boundary-

layer profile as in the case of Tollmien-Schilichting or cross-flow instability.

Appendix

$$a_{12}=a_{56}=a_{78}=1, \quad a_{21}=(U_x+\sigma U)/\mu\Theta+\beta^2$$

$$a_{22}=(V/\Theta-\mu_y)/\mu, \quad a_{23}=U_y/\mu\Theta$$

$$a_{25}=-[(UU_x+VU_y)/\Theta^2+(\tilde{\mu}U_y)_y]/\mu, \quad a_{26}=-\tilde{\mu}U_y/\mu$$

$$a_{31}=\Theta_x/\Theta-\sigma, \quad a_{33}=\Theta_y/\Theta, \quad a_{35}=(\sigma U+\chi-2Q/\Theta)/\Theta$$

$$a_{36}=V/\Theta, \quad a_{37}=-\beta$$

$$a_{41}=-\frac{1}{\Theta}[2UG^2+2\sigma(\mu\Theta)_y+c\sigma\mu\Theta_y]-\frac{1}{\Theta}\left[V_x+\frac{V\Theta_x}{\Theta}-\sigma V-(c+2)\left(\Theta_x\mu_y+\frac{\Gamma V\Theta_x}{\Theta}+\mu\Theta_{xy}\right)\right]$$

$$a_{42}=-\sigma\mu+\mu_x+(c+2)\frac{\mu}{\Theta}[\Theta_x-2(\tilde{\gamma}-1)M_\infty^2\Gamma VU_y]$$

$$a_{43}=-\frac{1}{\Theta}\left[\sigma U+\mu\Theta\beta^2+V_y+\frac{V\Theta_y}{\Theta}-(c+2)\left(\Theta_y\mu_y+\mu\Theta_{yy}+\frac{\Gamma V\Theta_y}{\Theta}\right)\right]$$

$$a_{45}=\frac{U^2G^2}{\Theta^2}+\sigma U_y\tilde{\mu}+\frac{(c+2)\sigma(\mu U)_y}{\Theta}+\frac{Q}{\Theta^3}[(c+2)(2\mu\Theta_y-\Gamma V)+2V]-\frac{2(c+2)(\mu Q)_y}{\Theta^2}+\chi\left[\frac{(c+2)\mu_y}{\Theta}-\frac{V}{\Theta^2}\right]+\frac{(c+2)}{\Theta}\left[\left\{\frac{\Gamma U\sigma}{\Theta}+\mu\beta^2-(\tilde{\gamma}-1)M_\infty^2\Gamma\tilde{\mu}(U_y)^2-\mu_{yy}\right\}V+\mu(U_{xy}+V_{yy})+\Theta(\tilde{\mu}V_y)_y\right]-\frac{UV\sigma}{\Theta^2}+c(\tilde{\mu}U_x)_y+(\tilde{\mu}U_y)_x+\frac{(UV_x+VV_y)}{\Theta^2}$$

$$a_{46}=\frac{(c+2)}{\Theta}\left[\mu\left(\sigma U+\chi-\frac{2Q}{\Theta}\right)+\frac{\Gamma V^2}{\Theta}-V\mu_y+\mu V_y\right]+\tilde{\mu}(c\chi+2V_y)-\frac{V^2}{\Theta^2}$$

$$a_{47}=-2\beta\mu_y+\frac{1}{\Theta}[\beta V-(c+2)\beta\mu\Theta_y], \quad a_{48}=-\beta\mu$$

$$a_{61}=\Gamma\Theta_x/\mu\Theta, \quad a_{62}=-2(\tilde{\gamma}-1)M_\infty^2\Gamma U_y, \quad a_{63}=\Gamma\Theta_y/\mu\Theta$$

$$a_{65}=\beta^2-\frac{\mu_{yy}}{\mu}+\frac{\Gamma}{\mu}\left[\frac{\sigma U}{\Theta}-\frac{Q}{\Theta^2}-(\tilde{\gamma}-1)M_\infty^2\tilde{\mu}(U_y)^2\right]$$

$$a_{66}=(\Gamma V/\Theta-2\mu_y)/\mu, \quad a_{81}=\beta[\mu_x/\mu+(c+1)\Theta_x/\Theta]$$

$$a_{83}=\beta[\mu_y/\mu+(c+1)\Theta_y/\Theta], \quad a_{84}=-\beta/\mu$$

$$a_{85}=\beta(c+1)(\sigma U+\chi-2Q/\Theta)/\Theta+c\tilde{\mu}\beta\chi/\mu$$

$$a_{86}=(c+1)\beta V/\Theta, \quad a_{87}=\beta^2+\sigma U/\mu\Theta, \quad a_{88}=(V/\Theta-\mu_y)/\mu$$

where

$$Q=V\Theta_y+U\Theta_x, \qquad \chi=U_x+V_y$$

Acknowledgment

This work was supported by NASA Langley Research Center under Grant NSG-1645.

References

[1] Kobayashi, R., "Note on the Stability of a Boundary Layer on a Concave Wall with Suction," *Journal of Fluid Mechanics*, Vol. 52, 1972, pp. 269-272.

[2] Kobayashi, R., "Stability of Laminar Boundary Layer on a Concave Permeable Wall with Homogeneous Suction," Tohoku University, Sendai, Japan, *Reports of the Institute of High Speed Mechanics*, Vol. 27, No. 253, 1973, pp. 31-47.

[3] Kobayashi, R., "Taylor-Görtler Instability of a Boundary Layer with Suction or Blowing," *AIAA Journal*, Vol. 12, 1974, pp. 394-395.

[4] Hughes, T. H. and Reid, W. H., "On the Stability of the Asymptotic Suction Boundary-Layer Profile," *Journal of Fluid Mechanics*, Vol. 23, 1965, pp. 715-735.

[5] Floryan, J. M. and Saric, W. S., "Stability of Görtler Vortices in Boundary Layers," *AIAA Journal*, Vol. 20, March 1982, pp. 316-324 (also AIAA Paper 79-1497, 1979).

[6] Floryan, J. M. and Saric, W. S., "Wavelength Selection and Growth of Görtler Vortices," AIAA Paper 80-1376, 1980.

[7] Diprima, R. C. and Dunn, D. W., "The Effects of Heating and Cooling on the Stability of Boundary-Layer Flow of Liquid over a Curved Surface," *Journal of Aeronautical Sciences*, Vol. 23, Oct. 1956, pp. 913-916.

[8] Kobayashi, R. and Kohama, K., "Taylor-Görtler Instability of Compressible Boundary-Layers," *AIAA Journal*, Vol. 15, Dec. 1977, pp. 1723-1273.

[9] El-Hady, N. M. and Verma, A. K., "Growth of Görtler Vortices in Compressible Boundary Layers along Curved Surfaces," AIAA Paper 81-1278, June 1981.

[10] Scott, R. R. and Watts, H. A., "Computational Solution of Linear Two-Point Boundary-Value Problems via Orthonormalization," *SIAM Journal of Numerical Analysis*, Vol. 14, 1977, pp. 40-70.

[11] Görtler, H., "Instabilität Laminarer Grenzchichten an Konkaven Wänden gegenüber gewissen Dreidimensionalen Störungen," *Zeitschriftfuer Angewandte Mathematik und Mechanik*, Vol. 21, No. 1, 1941, pp. 250-252 (see also NACA TM – 1375, 1954).

[12] Hämmerlin, G., "Zur Theorie der Dreidimensionalen Instabilität Laminarer Grenzschichten," *Zeitsehrift fuer Angewandte Mathematik und Physik*, Vol. 7, 1956, pp. 156-164.

[13] Kahawita, R. A. and Meroney, R. N., "The Influence of Heating on the Stability of Laminar Boundary Layers along Concave Curved Walls," *Journal of Applied Mechanics*, Vol. 44, 1977, pp. 11-17.

[14] Saric, W. S. and Nayfeh, A. H., "Non-Parallel Stability of Boundary-Layer Flows with Pressure Gradients and Suction," *Proceedings of AGARD Symposium on Laminar-Turbulent Transition*, AGARD CP-224, May 1977, Paper 6.

[15] El-Hady, N. M., "On the Stability of Three-Dimensional Compressible Nonparallel Boundary Layers," AIAA Paper 80-1374, 1980.

[16] Lekoudis, S., "The Stability of the Boundary Layer on a Swept Wing with Wall Cooling," AIAA Paper 79-1495, 1979.

[17] Mack, L. M., "Linear Stability Theory and the Problem of Supersonic Boundary-Layer Transition," *AIAA Journal*, Vol. 13, 1974, pp. 307-314.